Journal of Applied Polymer Science

# Mechanism of $M_xO_y$ nanoparticles/CNTs for catalytic carbonization of polyethylene and application to flame retardancy

**Karolina Wenelska,[1] Xuecheng Chen,[1,2] Beata Zielinska,[1] Ryszard J. Kaleńczuk,[1] Paul K. Chu,[3] Tao Tang,[2] Ewa Mijowska[1]**

[1]Institute of Chemical and Environment Engineering, Faculty of Chemical Technology and Engineering, West Pomeranian University of Technology, Szczecin 70-322, Poland

[2]State Key Laboratory of Polymer Physics and Chemistry, Changchun Institute of Applied Chemistry, Chinese Academy of Science (CAS), Changchun 130022, China

[3]Department of Physics and Materials Science, City University of Hong Kong, Kowloon, Hong Kong, China

Correspondence to: X. Chen (E-mail: xchen@zut.edu.pl) and T. Tang (E-mail: ttang@ciac.ac.cn) and P. K. Chu (E-mail: paul.chu@cityu.edu.hk)

**ABSTRACT:** Three kinds of metal oxide nanoparticles ($Fe_3O_4$, $Co_3O_4$, and $Ni_2O_3$) are produced on carbon nanotubes (CNTs). The synergistic effects rendered by the CNTs and metal oxide nanoparticles on carbonization of polyethylene (PE) are studied and applications to flame retardancy of PE are investigated systematically. The CNT-$Ni_2O_3$ delivers the best performance and the mechanism pertaining to the enhanced flame retardancy is proposed and discussed. It is found that under the same conditions, the carbonization rate can be a factor to influence the flame retardancy performance. Among Fe, Co, and Ni, Ni has the fastest carbonation rate, which leads to the best flame retardancy performance. © 2017 Wiley Periodicals, Inc. J. Appl. Polym. Sci. **2017**, *134*, 45233.

**KEYWORDS:** carbon nanotube; carbonization; flame retardant; metal oxide

Received 19 January 2017; accepted 18 April 2017
**DOI: 10.1002/app.45233**

## INTRODUCTION

Polyolefin-based products are used in cables, automobiles, electronic cases, interior decoration, packaging, and so on.[1–3] However, because of their inflammable nature, there is a considerable risk of fire-related injury and property loss and so the flame retardancy must be improved.[4] Traditional halogenated flame retardants are the most effective and widely used ones. However, owing to emission of toxic chemicals during burning, their use on a large scale is not suitable and they are actually banned in some countries.[5] Thus, an environment friendly flame retardant must be needed. During last decades, carbon nanotubes (CNTs) have been used as a flame retardant for polymers with small loading contents[6–11] because the CNT networks in the polymer matrix reduce the flammability of the nanocomposites also implying a close relationship between the viscoelastic characteristics and flammability properties.[12–16] Recently, carbonization is considered as an efficient way to improve the flame retardancy and thermal stability of polymers. Transformation of the polymer to carbonaceous materials can reduce the heat release rate (HRR) to stop the polymer from complete burning to $CO_2$ and the CNT network provides a thermal shield. For instance, Tang *et al.* have synthesized CNTs from polypropylene using a nickel catalyst (Ni or $Ni_2O_3$) to enhance the good flame retardancy[17] and Fe, Co, and Ni catalysts have been shown to be the most active in the formation of CNTs.[18] Hence, Fe, Co, Ni catalysts are considered as potential candidates as flame retardant for polymers. Until now, as far as we know, no reports have been published to compare them as flame retardants. In addition, graphitic carbon as a support for the metal catalyst can improve the carbon synthesis yield during chemical vapor deposition (CVD) because of the interaction between carbon and the metal catalyst.[19–21] Therefore, incorporation of CNTs with native flame retardancy and metal oxide nanoparticles can be the good choice and may further improve the flame retardancy of polymers.

In this work, polyethylene (PE)/CNT-$M_xO_y$ ($Fe_3O_4$, $Ni_2O_3$, and $Co_3O_4$) composites are prepared using the melt-mixing method. The CNTs in the polymer composite serves as a flame retardant,

Additional Supporting Information may be found in the online version of this article.

and improves the efficiency of PE carbonization. The metal oxide nanoparticles are the catalysts for carbonization of PE during combustion. The co-existence of CNT and metal oxide nanoparticles produces synergistic effects compared to a single component. The enhancement mechanism is proposed and discussed. Probably under the same conditions, the carbonization rate can be the critical factor to influence the flame retardancy performance. Among Fe, Co, and Ni, Ni has the fastest carbonation rate, which leads to the best flame retardancy performance.

## EXPERIMENTAL

### Materials

The PE used in this study was purchased from Sigma-Aldrich, Poland (PE, average $M_w$ ~4000, average $M_n$ ~1700) and the CNTs (10 nm in diameter), nickel(II) acetate tetrahydrate, iron (II) acetate, Cobalt (II) acetate tetrahydrate were bought from Sigma-Aldrich. The chemicals were used without further purification.

### Preparation of Polymer Nanocomposites

**Synthesis of CNT with Metal Oxide Nanoparticles (CNT-$M_xO_y$).** The different metal oxides were weighed and placed in a 50-mL beaker. The CNTs modified with metal oxide nanoparticles were prepared according to the following method. Briefly, 50 mg of CNT and 50 mg of metal oxide were dispersed in 150 mL of ethanol and sonicated for 24 h. Afterwards, the mixture was put in a furnace under vacuum of 1 mbar and dried at 440 °C before cooling to room temperature. Three different products: CNT-$Fe_3O_4$, CNT-$Co_3O_4$, and CNT-$Ni_2O_3$ labeled as CNT-Fe, CNT-Co, and CNT-Ni, respectively, were obtained.

**Synthesis of Metal Oxide Nanoparticles.** The metal acetate salts were put on a ceramic boat and inserted into a tube furnace and heated to 440 °C for 3 h. After cooling to room temperature, the samples were taken out.

**Preparation of Polymer Nanocomposites.** The CNTs and CNT incorporated with metal oxide nanoparticles were mixed with PE at different ratios by weight (1, 2, 3, and 10 wt %). The mixture was stirred mechanically at 160 °C and extrusion molded to form filaments with a diameter of 1 mm. The samples were labeled PE/CNT, PE/CNT-Fe, PE/CNT-Co, and PE/CNT-Ni.

### Carbonization of PE/CNT-Metal Oxide Composite

After the tube furnace was heated to 700 °C, the polymer composite was introduced and protected under Ar atmosphere. After 30 min, the tube furnace was cooled to the room temperature and the product was taken out for characterization.

### Characterization

The morphology was observed by transmission electron microscopy (TEM) and energy-dispersive X-ray spectroscopy (EDS) on the FEI Tecnai F20-based at 200 kV. Raman scattering using a 785 nm laser was conducted on the Renishaw Raman Microscope to determine the structure. Thermogravimetric analysis (TGA) was performed on the DTA-Q600 SDT to determine the mass changes during heating as a function of temperature in air. X-ray diffraction (XRD, Philips X'Pert PRO) was carried out to determine the phase composition. The combustion behavior was monitored on the FTT Micro Calorimeter according to the Federal Aviation Administration (FAA) requirements to acquire the thermo-chemical data.

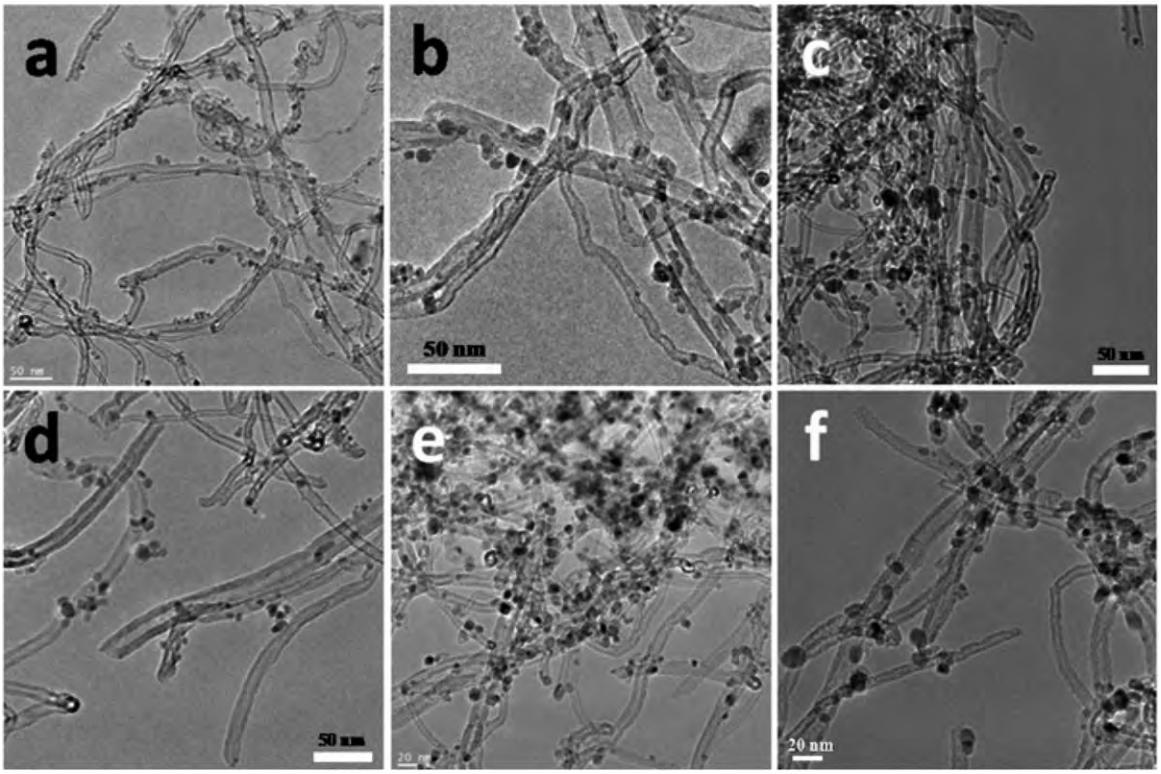


**Figure 1.** TEM images: (a,b) CNT-$Fe_3O_4$, (c,d) CNT-$Co_3O_4$, and (e,f) CNT-$Ni_2O_3$.

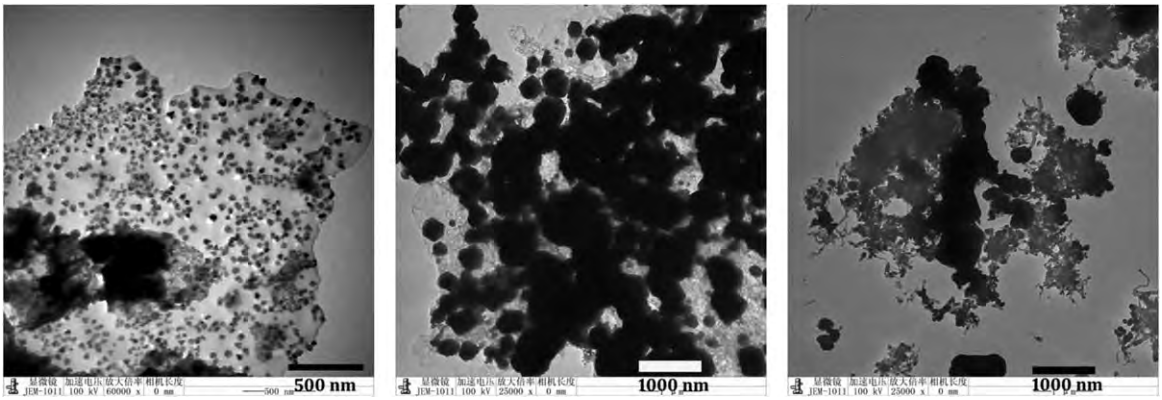


**Figure 2.** TEM images: (a) $Fe_3O_4$, (b) $Co_3O_4$, and (c) $Ni_2O_3$ nanoparticles obtained by pyrolysis of iron acetate, cobalt acetate, and nickel acetate, respectively, under Ar at 440 °C.

## RESULTS AND DISCUSSION

Figure 1 depicts TEM images of the CNTs decorated with metal oxides nanoparticles [Figure 1(a,b) CNT-$Fe_3O_4$, Figure 1(c,d) CNT-$Ni_2O_3$, and Figure 1(e,f) CNT-$Co_3O_4$] showing that the metal oxide nanoparticles have been incorporated into the CNTs. The diameter of the CNTs is about 10 nm and the CNTs decorated with iron oxide nanoparticles have a diameter between 4 and 20 nm [Figure 1(a,b) and Supporting Information Figure S3]. The diameters of CNT-$Co_3O_4$ and CNT-$Ni_2O_3$ are 6–22 nm [Figure 1(c,d) and Figure S3] and 6–17 nm [Figure 1(e,f) and Supporting Information Figure S3], respectively. The weight percentages of metal oxide nanoparticles evaluated by TGA (Supporting Information Figure S1) were found to be 30, 44, 16 wt % for $Fe_3O_4$, $Co_3O_4$, and $Ni_2O_3$ on the CNTs, respectively. The XRD patterns of the metal oxide nanoparticles in Supporting Information Figure S2 reveal the presence of $Fe_3O_4$, $Co_3O_4$, and $Ni_2O_3$.

In order to study the role of CNTs in the preparation of the CNT-metal oxide nanocomposites, pure metal oxide is prepared as the control. Figure 2 shows that without the CNT support, metal acetate decomposes and agglomerates in Ar in the case of iron and cobalt acetate and only big particles are found. The size of the $Fe_3O_4$ particles is between 20 and 100 nm but $Co_3O_4$ is bigger than $Fe_3O_4$ [Figure 2(a,b)]. However, for nickel acetate, after pyrolysis at 440 °C in Ar, several carbon nanofibers (CNFs) can be observed [Figure 2(c)] showing the existence of $Ni_2O_3$. A low reaction temperature favors the formation of CNFs rather than CNTs. In carbonization of organic species, $Ni_2O_3$ yields the best results even at a low decomposition temperature of 440 °C. This observation and Figure 1 confirm that the CNTs help to disperse the metal oxide nanoparticles and preclude aggregation of the metal oxide to become nanoparticles.

Table I shows the results of the initial pyrolyzed experiments. In order to obtain the best flame retardant properties, the pyrolyzed experiments are performed at 700 °C under Ar and the weight percentage of the added CNTs and CNT-$M_xO_y$ is 10 wt %. With regard to pure PE without adding a flame retardant, no residual carbon is formed. When 10 wt % of CNTs are added, 12.5 wt % of the residue is left, meaning that 2.5 wt % of new carbon is formed with the help of CNTs. When CNTs are decorated with metal oxide nanoparticles, carbon formation is even more efficient. In the PE mixtures with carbon nanotubes decorated by $Fe_3O_4$, $Co_3O_4$, and $Ni_2O_3$, the yields of residual char are 21.7, 29.8, and 36.3 wt % for PE/CNT-$Fe_3O_4$, PE/CNT-$Co_3O_4$, and PE/CNT-$Ni_2O_3$, respectively, after combustion at 700 °C, suggesting that metal oxides catalyze carbonization of the PE. Based on the amount of metal oxide nanoparticles on the CNTs (Supporting Information Figure S1), the same amount of metal oxide is mixed with PE without the CNT support and the corresponding char yields are 2.6, 5.2, and 3.8 wt %, which are smaller than those of CNT-$M_xO_y$. Hence, the metal oxide and CNT enhance carbonization of PE and CNT-$Ni_2O_3$ delivers the best performance. During pyrolysis, $Ni_2O_3$ can better catalyze the process than the other two catalysts.[22]

The polymers show the 110 and 220 diffraction peaks[23] in the XRD patterns in Supporting Information Figure S4 which also discloses the crystallinity of the PE/CNT, PE/CNT-$Fe_3O_4$, PE/CNT-$Ni_2O_3$, and PE/CNT-$Co_3O_4$ composites. The crystallinity of PE in all the samples decreases after addition of CNTs because the metal oxide particles interfere with crystallization of PE. The largest decrease in the intensity of the peak at 22° (2θ) is observed from PE/CNT-$Ni_2O_3$. The PE/CNT-$M_xO_y$ composites are also characterized by Raman scattering (Supporting

**Table I.** Char Yields of PE/CNT-$M_xO_y$ (10 wt %) Pyrolyzed at 700 °C in Ar

| Sample | Yields of residual char (%) | Carbon produced (%) |
|---|---|---|
| PE | 0 | 0 |
| PE/CNT(10 wt %) | 12.5 | 2.5 |
| PE/CNT-$Fe_3O_4$ (10 wt %) | 21.7 | 11.7 |
| PE/CNT-$Co_3O_4$ (10 wt %) | 29.8 | 19.8 |
| PE/CNT-$Ni_2O_3$ (10 wt %) | 36.3 | 26.3 |
| PE/$Fe_3O_4$ (3 wt %) | 2.6 | 0 |
| PE/$Co_3O_4$ (4.4 wt %) | 5.2 | 1.2 |
| PE/$Ni_2O_3$ (1.6 wt %) | 3.8 | 0 |

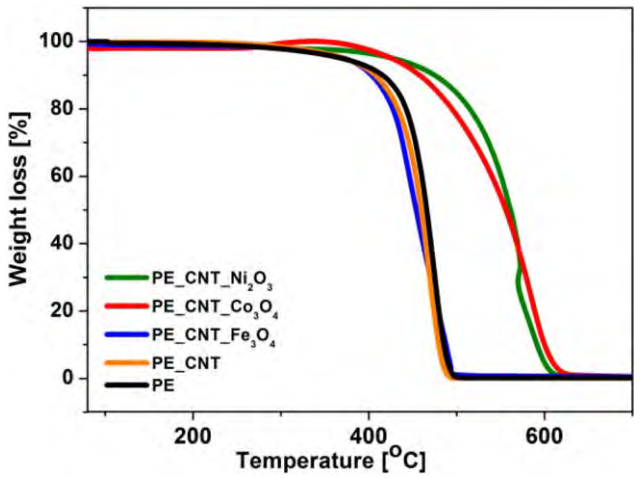


**Figure 3.** TGA profiles of PE, PE/CNT, PE/CNT-$Fe_3O_4$, PE/CNT-$Co_3O_4$, and PE/CNT-$Ni_2O_3$. [Color figure can be viewed at wileyonlinelibrary.com]

Information Figure S5), which proves the existence of metal oxide and CNTs.

The thermal stability of the polymer composites is monitored by TGA in air (Figure 3). The degradation temperature of PE and PE/CNT is 438 and 431 °C, respectively, and introduction of CNTs lowers the thermal stability of PE. However, for CNT-$Ni_2O_3$, the decomposition temperature increases to 511 °C which is higher than that of PE. The presence of PE/CNT-$Ni_2O_3$ in the PE matrix enhances the thermal stability. The decomposition temperature of PE/CNT-$Fe_3O_4$ and PE/CNT-$Co_3O_4$ is 415 and 495 °C, respectively. The thermal stability of PE/CNT-$Fe_3O_4$ is even lower than that of PE and PE/CNT. In the case of PE/CNT-$Co_3O_4$, the thermal stability is higher than PE.

The flammability of the polymer composites is assessed on a microcombustion calorimeter. The heat of combustion of the pyrolysis products is measured and the heat released is used to determine the flammability of the materials. The HRR is one of the important parameters to characterize combustion. The HRR curves of the samples are shown in Figure 4 and the corresponding data are listed in Supporting Information Table S1. The pristine PE burns very fast showing the largest heat release rate (PHRR) of 1215 W/g. When CNTs are added as flame retardants, the PHRR decreases and when CNT-$M_xO_y$ is added, the PHRR diminishes further. The PHRR values of PE/CNT-$Ni_2O_3$_1%, PE/CNT-$Ni_2O_3$_3%, and PE/CNT-$Ni_2O_3$_10% are 875, 728, and 575 W/g, respectively.

The larger the CNT- $Ni_2O_3$ content in the polymer composite, the smaller are the PHRR peak values. Enhanced flame retardant properties are also observed from the polymer composites with CNT-Fe and CNT-$Co_3O_4$. For example, when 10 wt % of flame retardant is added to the PE, the PHRR values PE,

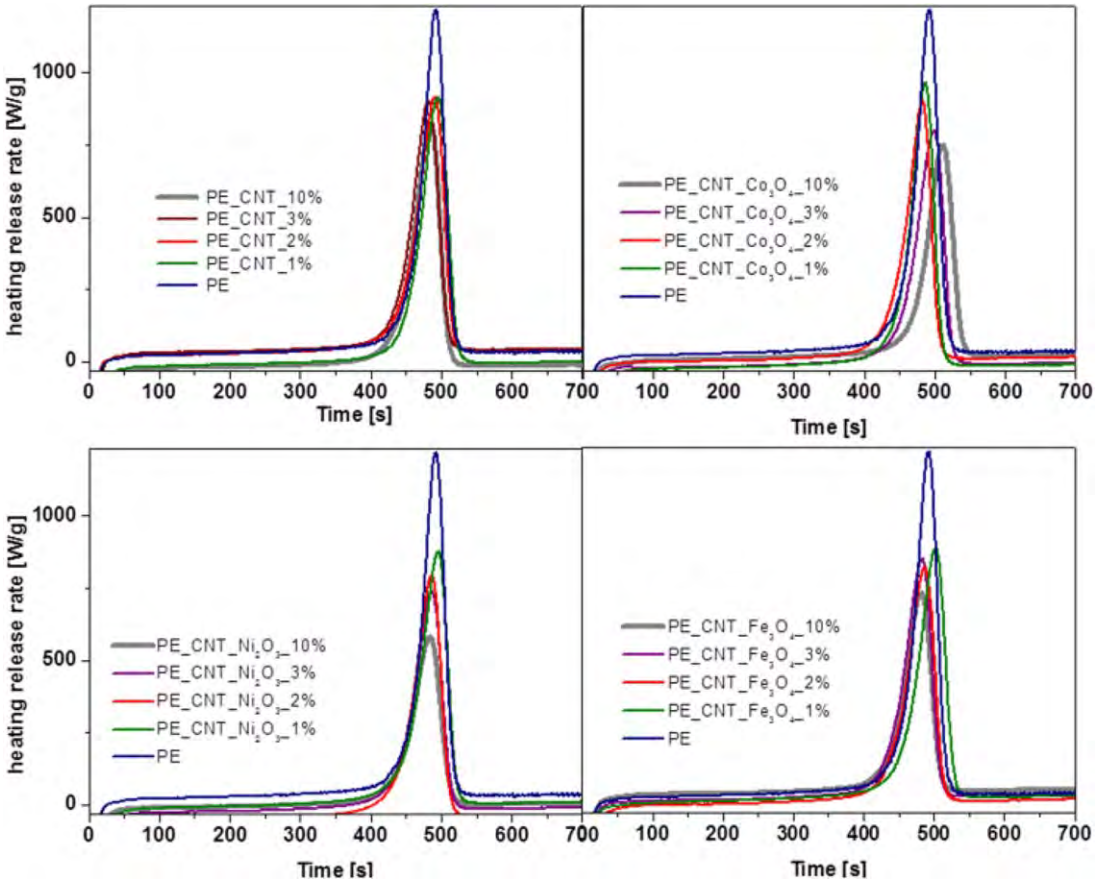


**Figure 4.** HRR curves: (a) PE/CNT, (b) PE/CNT-$Co_3O_4$, (c) PE/CNT-$Ni_2O_3$, and (d) PE/CNT-$Fe_3O_4$. [Color figure can be viewed at wileyonlinelibrary.com]

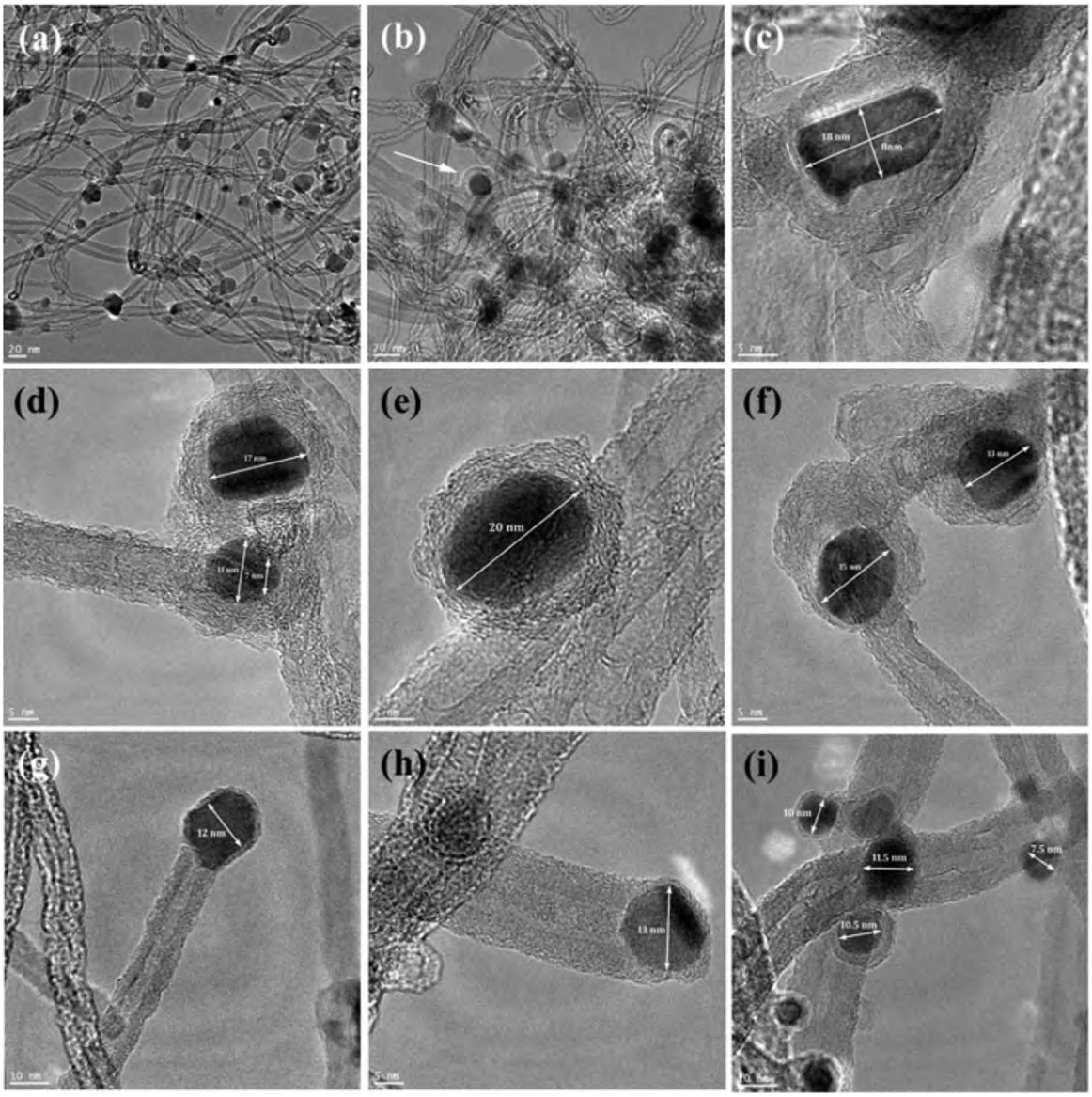


**Figure 5.** TEM images: (a–c) PE/CNT-$Fe_3O_4$, (a–c), (b-f) PE/CNT-$Co_3O_4$, and (g–i) PE/CNT-$Ni_2O_3$ after annealing at 700 °C in Ar.

PE/CNT, PE/CNT-$Fe_3O_4$, PE/CNT-$Co_3O_4$, and PE/CNT-$Ni_2O_3$ are 1215, 823, 741, 728, and 575 W/g, respectively. CNT-$Ni_2O_3$ gives the smallest PHRR value, CNT-$Co_3O_4$ is a little bigger than that of CNT $Ni_2O_3$, and that of CNT-$Fe_3O_4$ is larger than that of CNT-$Co_3O_4$. Supporting Information Table S1 presents the PHRR data of the three kinds of CNT-metal oxides/polymer composites showing that CNT-$Ni_2O_3$ is the best flame retardant. The CNT and metal oxide after carbonization of PE leads to synergistic effects. Metal oxide on CNTs catalytically changes the PE into carbon materials more efficiently and leads to lower PHRR values as consistent with the data in Table I.

In order to investigate the flame retardancy mechanism of the different metal oxide nanoparticles, the pyrolyzed products are characterized by TEM. Figure 5 displays the TEM images of the carbon products after pyrolysis of PE/CNT-$Fe_3O_4$, PE/CNT-$Co_3O_4$, and PE/CNT-$Ni_2O_3$ at 700 °C in Ar. In all the three samples, both of CNTs and carbon particles are found. Most of $Fe_3O_4$ nanoparticles in PE/CNT-$Fe_3O_4$ after pyrolysis have the same morphology as before. The size of the $Fe_3O_4$ nanoparticle is in the range of 6.5–20 nm [Figure 5(a)] and some $Fe_3O_4$ nanoparticles are coated by carbon as indicated by white arrow in Figure 5(b), indicating that only a small fraction of the $Fe_3O_4$ nanoparticles take part in the carbonization reaction of PE. It is noted that the coated carbon on $Fe_3O_4$ particle has the graphitic structure [Figure 5(c)]. After pyrolysis experiment, some large $Co_3O_4$ nanoparticles appear from PE/CNT-Co, indicating coalescence and reshaping of the $Co_3O_4$ particles during pyrolysis as shown in Supporting Information Figure S7. CNTs and carbon-coated $Co_3O_4$ nanoparticles are found [Figure 5(d–f)]. In the coated $Co_3O_4$ particle CNT, the diameter of $Co_3O_4$ is smaller than 11 nm [Figure 5(d)]. However, if the $Co_3O_4$ nanoparticles are larger than 17 nm, carbon-coated $Co_3O_4$ nanoparticles are found [Figure 5(d,e)], meaning that the growth of CNT is catalyst-size dependent and only $Co_3O_4$ nanoparticles

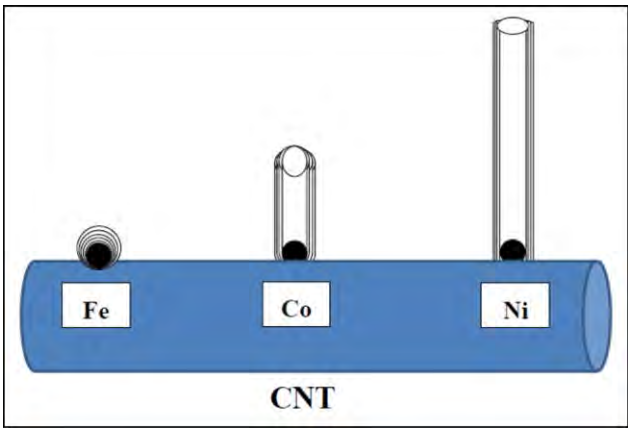


**Figure 6.** Illustration of the metal oxide ($Fe_3O_4$, $Co_3O_4$, $Ni_2O_3$) catalysts on the CNT during carbonization of PE to carbon nanostructures. [Color figure can be viewed at wileyonlinelibrary.com]

with the optimal size can induce the growth of CNTs. The crystallinity of the carbon coat on $Co_3O_4$ is worse than that on $Fe_3O_4$ [Figure 5(e)]. With regard to PE/CNT-$Ni_2O_3$, CNFs are found next to CNT and carbon-coated $Ni_2O_3$ nanoparticles (Supporting Information Figure S8). Growth of CNFs may be induced by larger $Ni_2O_3$ nanoparticles.[24] According to the TEM images in Figure 5(i) and Supporting Information Figure S8, almost all of the $Ni_2O_3$ nanoparticles are coated by carbon. The large $Ni_2O_3$ particles are attributed to agglomeration of small $Ni_2O_3$ nanoparticles (Supporting Information Figure S8). The diameter of $Ni_2O_3$ is in the range of 7–13 nm, which is bigger than the $Co_3O_4$ nanoparticles [Figure 5(g,h)], indicating that more CNTs can be produced from this sample than that containing $Co_3O_4$. The images in Figure 5(g,h) reveal $Ni_2O_3$ particles at the tip of the CNT indicative of a tip-based growth mechanism. It has been suggested that the strong interaction between the supporting materials and metal would form CNTs without the metal, whereas a weak interaction produces CNTs filled with metal particles.[22,25] Small $Ni_2O_3$ nanoparticles (7.5–10.5 nm) are observed to be coated by carbon [Figure 5(i)] and it may occur in the early stage of CNT growth. It is also noted that the crystallinity of the carbon coat on $Ni_2O_3$ is poor.

According to the TEM images, it can be proposed that more carbon can be produced in the presence of CNT-$Ni_2O_3$ than CNT-Fe or CNT-Co. This is because more $Ni_2O_3$ nanoparticles are involved in the carbonization process when the polymer is pyrolysed, whereas only few $Fe_3O_4$ and $Co_3O_4$ nanoparticles take part in carbonization of PE. Hence, at a certain time (the time for polymer combustion to diminish), the carbonation rate of $Ni_2O_3$ is the fastest. The fast carbonization rate leads to more carbon and less carbon is produced by $Ni_2O_3$ nanoparticles than the $Co_3O_4$ and $Fe_3O_4$. This is consistent with the previous results that Ni catalyze the formation of CNTs faster than $Co_3O_4$ and Fe (Figure 6).[26] It is reasonable to infer that more carbon produced *in situ* from the polymer reduce heat released to the air leading to the HRR peak decrease.[17] The combustion experiments and HRR measurements show that CNT-$Ni_2O_3$ delivers the best performance with CNT-$Fe_3O_4$ behaving the worst and CNT-$Co_3O_4$ in the middle. This can be ascribed to the different carbonization efficiency of the three CNTs-$M_xO_y$ in the PE matrix. The best synergistic effects are observed from CNT and $Ni_2O_3$ resulting in more efficient carbonization of PE to CNTs and the best flame retardancy (Figure 6).

## CONCLUSIONS

Addition of CNTs-$M_xO_y$ to PE decreases the PHRR and retards combustion. The improved flame retardancy is attributed to the existence of CNTs in the polymer matrix and carbonization of the degradation products of PE catalyzed by $Ni_2O_3$, $Co_3O_4$, and $Fe_3O_4$. It also shows that the carbonization rate determines the flame retardancy performance, which means more carbon would be produced during combustion process, fast carbonization rate leads to good flame retardancy performance, such as Ni nanoparticles. The combination of CNTs with carbonization catalysts is a promising strategy to simultaneously improve the flame retardancy as well as of polymeric materials.

## ACKNOWLEDGMENTS

The authors are grateful for the financial support of National Science Centre, Poland, grant No. 2011/03/D/ST5/06119 and City University of Hong Kong Applied Research Grant (ARG) No. 9667104.

## REFERENCES

1. Li, Q.; Jiang, P. K.; Su, Z. P.; Wei, P.; Wang, G. L.; Tang, X. Z. *J. Appl. Polym. Sci.* **2005**, *96*, 854.
2. Wang, X. Y.; Li, Y.; Liao, W. W.; Gu, J.; Li, D. *Polym. Adv. Technol.* **2008**, *19*, 1055.
3. Lv, P.; Wang, Z. Z.; Hu, K. L.; Fan, W. C. *Polym. Degrad. Stab.* **2005**, *90*, 523.
4. Le Bras, M.; Bgajny, M.; Lefebvre, J. M.; Bourbigot, S. *Polym. Int.* **2000**, *49*, 115.
5. Xie, R. C.; Qu, B. J. *J. Appl. Polym. Sci.* **2001**, *80*, 1181.
6. Kashiwagi, T.; Du, F.; Douglas, J. F.; Winey, K. I.; Harris, R. H.; Shields, J. R. *Nat. Mater.* **2005**, *4*, 928.
7. Kashiwagi, T.; Grulke, E.; Hilding, J.; Groth, K.; Harris, R.; Butler, K.; Shields, J.; Kharchenko, J.; Douglas, J. *Polymer* **2004**, *45*, 4227.
8. Kashiwagi, T.; Du, F.; Winey, K. I.; Groth, K. M.; Shields, J. R.; Bellayer, S. P.; Kim, H.; Douglas, J. F. *Polymer* **2005**, *46*, 471.
9. Jiang, Z. W.; Song, R. J.; Bi, W.; Lu, J.; Tang, T. *Carbon* **2007**, *45*, 449.
10. Wen, X.; Wang, Y.; Gong, J.; Liu, J.; Tian, N. N.; Wang, Y. H.; Jiang, Z. W.; Qiu, J.; Tang, T. *Polym. Degrad. Stab.* **2012**, *97*, 793.
11. Yu, H.; Jiang, Z. W.; Gilman, J. W.; Kashiwagi, T.; Liu, J.; Song, R. J.; Tang, T. *Polymer* **2009**, *50*, 6252.
12. Cao, L.; Su, D. F.; Su, Z. Q.; Chen, X. N. *Ind. Eng. Chem. Res.* **2014**, *53*, 2308.
13. Pang, H.; Yan, D. X.; Bao, Y.; Chen, J. B.; Chen, C.; Li, Z. M. *J. Mater. Chem.* **2012**, *22*, 23568.

14. Zhang, X. H.; Liang, G. Z.; Chang, J. F.; Gu, A. J.; Yuan, L.; Zhang, W. *Carbon* **2012**, *50*, 4995.

15. Yu, H.; Liu, J.; Wen, X.; Jiang, Z. W.; Wang, Y.; Wang, L.; Zheng, J.; Fu, S. Y.; Tang, T. *Polymer* **2011**, *52*, 4891.

16. Gong, J.; Liu, J.; Ma, L.; Wen, X.; Chen, X. C.; Wan, D.; Yu, H.; Jiang, Z. W.; Borowiak-Palen, E.; Tang, T. *Appl. Catal. B* **2012**, *117–118*, 185.

17. Tang, T.; Chen, X. C.; Chen, H.; Meng, X. Y.; Jiang, Z. W.; Bi, W. G. *Chem. Mater.* **2005**, *17*, 2799.

18. Biró, L. P.; Bernardo,C. A.; Tibbetts, G. G.; Lambin, Ph.; Eds. Carbon Filaments and Nanotubes: Common Origins, Differing Applications? Kluwer Academic Publishers: The Netherlands, **2001**; p 85.

19. Otsuka, K.; Abe, Y.; Kanai, N.; Kobayashi, Y.; Takenaka, S.; Tanabe, E. *Carbon* **2004**, *42*, 727.

20. Pham-Huu, C.; Vieira, R.; Louis, B.; Carvalho, A.; Amadou, J.; Dintzer, T.; Ledoux, M. J. *J. Catal* **2006**, *240*, 194.

21. Sohn, J. R.; Cho, E. S. *Appl. Catal. A Gen.* **2005**, *283*, 147.

22. Eren, B.; Marot, L.; Steiner, R.; Arcos, T.; Marcel Düggelin, M.; Mathys, D.; Goldie, K. N.; Olivieri, V.; Meyer, E. *Chem. Phys. Lett.* **2014**, *609*, 82.

23. Alsaygh, A. A.; Al-hamidi, J.; Alsewailem, F. D.; Al-Najjar, I. M.; Kuznetsov, V. L. *Appl. Petrochem. Res.* **2014**, *2*, 79.

24. Zhao, Y.; Li, C. H.; Yao, K. F.; Jiang, J. *J. Mater. Sci.* **2007**, *42*, 4240.

25. Zhang, T. J.; Amiridis, M. D. *Appl. Catal. A Gen.* **1998**, *167*, 161.

26. Li, Y. H.; Gao, H. Q.; Yang, J. H.; Gao, W. L.; Xiang, J.; Li, Q. Y. *Mater. Sci. Eng. B: Solid State Mater. Adv. Technol.* **2014**, *187*, 113.